

EFFECTIVENESS OF MICRO-PILE INSTALLATION CONFIGURATION FOR INCREASING THE ULTIMATE SHALLOW FOUNDATION BEARING CAPACITY ON SOFT CLAY SOIL

*Isnaniati¹, Indrasurya B Mochtar², and Noor Endah Mochtar³

^{1,2,3} Civil Engineering Department, Institute Technology of Sepuluh Nopember, Surabaya, Indonesia

¹ Civil Engineering Department, Muhammadiyah University, Surabaya, Indonesia

*Corresponding Author, Received: 23 Nov. 2023, Revised: 09 March 2024, Accepted: 13 March 2024

ABSTRACT: Soft clay soil is known for low bearing capacity and is prone to soil collapse under shallow foundations through Local Shear Failure. An approach to enhance the load-bearing capacity of such soil is by adopting micro-piles as reinforcement. This study aims to determine the effectiveness of micro piles in strengthening shallow foundations on soft clay soil through laboratory-scale testing. The soft soil used comes from kaolin clay characterized by a cohesion (c_u) of 20.692 kN/m² and water content (w_c) of 58.631%. These properties guided the crafting of test specimens, formed with a diameter (d_s) of 0.33m and a height (H_s) of 0.185m. Micro-piles were constructed from bamboo with varying numbers ($n = 4, 9, 16, 25$), lengths ($L_1 = 1.33B$, $L_2 = 1.73B$, $L_3 = 2.13B$), and diameters ($d_1 = 0.03B$, $d_2 = 0.04B$, $d_3 = 0.07B$). The shallow foundation model with a square shape of $B \times B$ (where $B = 0.075$ m), incorporated diverse configurations for the installation of micro-piles (K_1 , K_2 , K_3). The results showed that more micro-piles (n) led to a higher bearing capacity ratio at a 0.1B reduction ($R_{q_{ult-mp}}$). The most significant enhancements occurred with the longest micro-piles ($L_3 = 2.13B$), the highest number ($n_4 = 25$), and a diameter of 0.04 B. Additionally, configurations including micro-piles installed beneath and extending up to the foundation's edge (K_1 and K_2) exhibited significant enhancement in $R_{q_{0.1B}}$ for identical micro-piles numbers (n). The installation of micro-piles beyond the foundation perimeter did not yield substantial increases in $R_{q_{0.1B}}$ and, therefore, is not recommended.

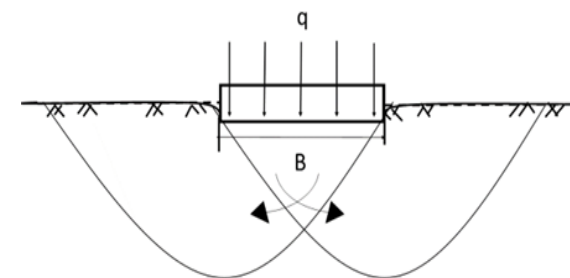
Keywords: Local Shear Failure, Laboratory-Scale Model, Micro-Pile Reinforcement, Shallow Foundation, Soft Clay Soil.

1. INTRODUCTION

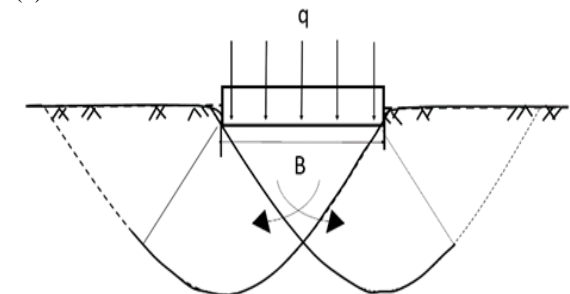
The existence of two types of shear failure, namely general or total and local shear failure, is asserted by Terzaghi et al. [1,2]. Total shear failure occurs when the collapse plane reaches the surface, causing the soil on either side of the foundation to protrude, as shown in Fig.1a. This form of failure is dictated by the maximum stress exerted on the structure. Conversely, local shear failure is characterized by triangular blocks failing beneath the foundation, which moves downward and ends somewhere within the soil, as shown in Fig. 1b. This type of failure is characterized by the maximum deformation that occurs within the soil. With the soft soil sample used in this study, the analysis is grounded on Local Shear Failure as the fundamental basis.

Installing micro-piles that penetrate through the zone of shear failure is an effective strategy for enhancing the load-bearing capacity of the soil beneath shallow foundations. This method has been explored extensively by various scholars and applied to enhance the load-bearing capacity of the soil beneath shallow foundations [3-9]. Additionally, micro-pile reinforcement has been proposed by Rusdiansyah et al. [10,11] to increase the shear strength of the soft soil beneath the embankment. The

degree of improvement in soil shear strength achieved through micro-pile reinforcement is strongly influenced by the ratio of pile thrust and spacing between micro-piles.



(a) General Shear Failure



(b) Local Shear Failure

Fig.1 Failure patterns of soil bearing capacity in shallow foundations, reproduced based on [1,2].

An increase in shear resistance occurs when the spacing between the micro-piles ranges from 3D to 5D, as stated by Rusdiansyah, et al. [10]. Additionally, the study [11] also states an enhancement in shear resistance with an increased number of piles. The orientation of micro-pile installation significantly impacts the load-bearing capacity, with the vertical direction ($\theta = 0^\circ$) on clay and sand exhibiting the maximum increase in bearing ability. This increase diminishes as the installation angle deviates from the vertical ($\theta > 0^\circ$), as indicated by Tsukada Y et al. [3].

The findings correlate with the research by Abbas et al [12], who observed that installing micro-piles on rocky soil with a steeper slope ($\theta > 0^\circ$) leads to a reduced increase in bearing capacity. The laboratory-scale study conducted by Suroso et al [4] found that variations in micro-piles diameter and length resulted in an average bearing capacity increase of approximately 2.2 times of the initial soil.

Numerical methods, particularly the finite element method (FEM), have been used to investigate the effect of placement patterns, such as Micro-Piles Groups (MPG) and Single Micro-Piles (MPS), in sandy and clay soil layers. Alnuaim et al. [5, 6] show that the MPG placement pattern yields a greater increase in total carrying capacity (q_{ult}) compared to the MPS pattern in both soil types. Hasheminezhad et al. [9] found that numerical research using FLAC3D on deep soil mixing (DSM) shows seismic carrying capacity increases with longer DSM, but larger DSM diameters decrease the bearing capacity of shallow foundations.

Beyond the separate laboratory and numerical research, simultaneous studies have also been conducted using GeoStudio 2D element analysis. These investigations focus on micro-piles as reinforcement for soft soil mixed with fly ash beneath shallow foundations. The study, varying the ratio of micro-piles length to diameter ($L/D = 60, 80, 100, 120$), consistently shows higher bearing capacity ratio values compared to those reported by Shah et al. [8].

Field study on post-grouting micro-poles in soft soil is presented as a case study including inclined transmission towers in China. Wen et al. [7] report a significant increase in the bearing capacity of axial piles, reaching 2.5 times the capacity of micro-piles without grouting.

Based on previous research, the study progresses to evaluate the augmentation in the total bearing capacity of shallow foundations through the installation of micro-piles with varying numbers (n), lengths (L), diameters (d), and installation configurations (k). The medium for this investigation is provided by soft clay soil, with a square foundation layout. The ensuing discussion will include the following findings.

1. The impact of micro-pile numbers in increasing the ultimate bearing capacity of shallow

foundations.

2. The influence of micro-pile lengths in the augmentation of the ultimate bearing capacity of shallow foundations.
3. The role of micro-pile diameters in enhancing the ultimate bearing capacity of shallow foundations.
4. The significance of micro-pile installation configuration in amplifying the ultimate bearing capacity of shallow foundations.

This contribution of the study lies in elucidating the correct micro-pile installation practices to achieve a substantial increase in ultimate bearing capacity (q_{ult}) post-installation. It provides valuable insights for engineering projects reliant on shallow foundation systems.

2. RESEARCH SIGNIFICANCE

The significance of this study focused on the understanding of the type of soil failure beneath shallow foundations, enabling the strategic installation of micro-piles within the failure zone (K). This ensured that micro-piles served the purpose of reinforcement, effectively enhancing the ultimate bearing capacity (q_{ult}) of soft clay soil. Proper installation of micro-piles was essential to intersect the failure zone, thereby augmenting shear strength and eventually increasing q_{ult} .

3. VARIABLE AND METHODS

3.1 Variable

The materials used in this study comprised clay with the consistency level of soft clay and micro-piles crafted from apus bamboo (*Gigantochloa*) [Bahtiar et al. 13, 14], with a tensile strength (σ_{lt}) of 382459.3 kN/m². The apus bamboo used in the study had been aged for a minimum of two years [15]. The micro-piles were formed with diameters of $d_1 = 0.03B$, $d_2 = 0.04B$, $d_3 = 0.07B$, lengths of $L_1 = 1.33B$, $L_2 = 1.73B$, $L_3 = 2.13B$, and varying cones numbers of $n_1 = 4$, $n_2 = 9$, $n_3 = 16$, $n_4 = 25$. The micro-piles configurations included $K_1 = 0.67B$, $K_2 = 1.0B$, and $K_3 = 1.33B$, with the installation model depicted in Figs. 2-4.

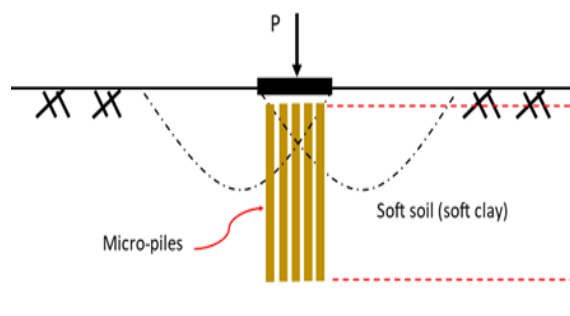


Fig.2. Micro-piles installed under the foundation (K_1).

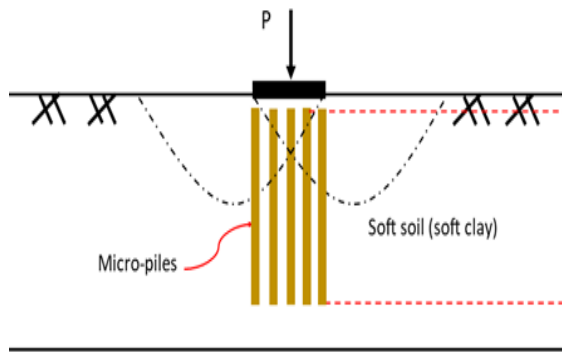


Fig.3 Micro-piles installed to the foundation's edge (K_2).

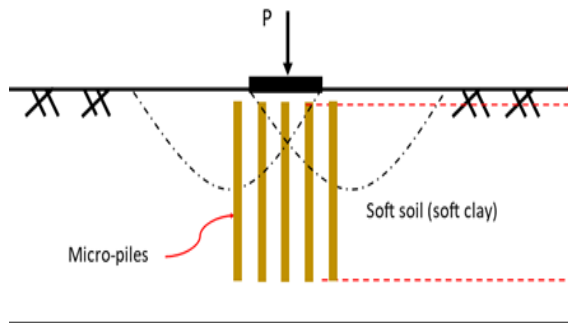


Fig.4 Micro-piles installed outside the foundation (K_3).

The study comprising variations in diameter, length, number, and configuration of the micro-piles progressed through three stages, namely.

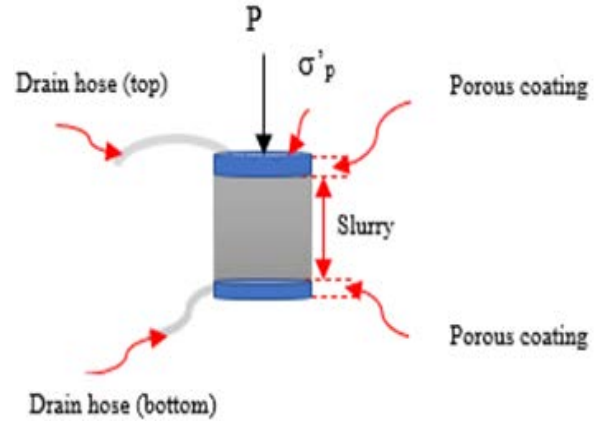
- Preparation of test objects comprised of shaping soft clay specimens.
- The subsequent stage comprised inserting cones into the test objects.
- Testing of the test objects followed.

The results of this study consisted of the ratio (R_q) between the ultimate bearing capacity at 0.1B settlement and under local shear conditions without micro-piles, as defined by Terzaghi ($R_q = Q_{ult-empirical} / Q_{ult-local\ shear\ Terzaghi}$).

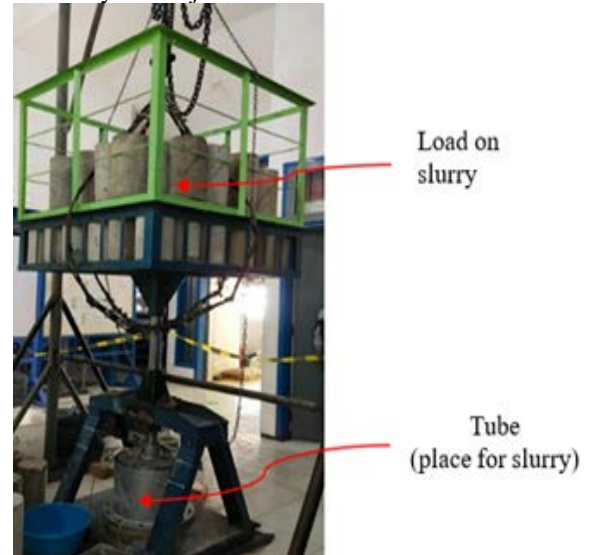
3.2 Manufacture of Test Objects

Clay with a soft consistency was achieved by preparing a slurry from kaolin powder sourced at Bangka Island, Indonesia, with a liquid limit value (LL) of 62 and plastic limit (PL) of 38. Following the recommendation of Lambe. T.W [16], the slurry's water content (w_c) was set at 1.7LL. Brown [17] specified pouring the slurry into a tube with a diameter (d) of 33 cm. To achieve the planned specimen characteristics (c_u) of 0.211 kg/cm² and a water content (w_c) of 58.631%, the slurry needed to be subjected to an effective stress load (σ'_p) of 114,149 kN/m² over a timeframe (t) of 5 to 7 days. In this laboratory study, a 1/30 scale was adopted, consistent with the field scale used by Alfani et al [18,

19]. The resulting clay soil test object, obtained through loading, had a diameter (d_s) of 0.33 m and a height (H_s) of 0.185 m. The loading process of the slurry is visually represented in Fig. 5.



(a) The arrangement of the drainage layers in the slurry test object tube.



(b) Compressing the slurry until a test object with a soft consistency was obtained.

Fig.5 Making a soft clay specimen with a diameter of 0.33m.

3.3 Installation of Micro-Piles into the Test Object

The positioning during micro-pile installation significantly influences the extent of the increase in ultimate bearing capacity and requires careful consideration, as observed by Issakulov et al. [20]. These micro-piles were positioned beneath a square plate foundation [21] measuring 0.075 x 0.075 m², which was centered within the clay specimen with a diameter (d) of 0.33 m. The configuration of micro-piles installation, including K_1 , K_2 , and K_3 as reinforcement, played a crucial role in determining the extent of the increase in ultimate bearing capacity [Munawir et al. 22], particularly evident in Figure 4

for a total of 25 micro-piles ($n_4=25$). K represented the distance of outermost micro-piles, with $K_1=0.67B$, $K_2=B$, and $K_3=1.33B$, where B denoted the width of the foundation.

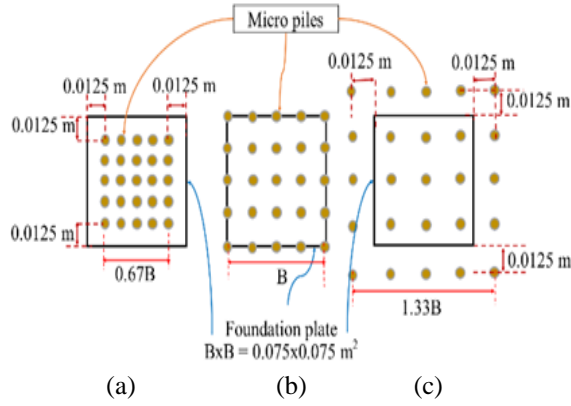


Fig.6 Configuration of the installation of micro-piles for the number $n_4 = 25$. (a) The micro-piles were installed beneath the foundation ($K_1=0.67B$). (b) The micro-piles were installed at the edge of the foundation ($K_2= B$). (c) The micro-piles were installed outside the foundation ($K_3= 1.33B$).

Ensuring the tips of the micro-piles were pointed was crucial in minimizing structural damage between soil grains caused by their installation into the soil specimen. Additionally, the micro-piles had to be inserted in an upright position ($\theta = 0^\circ$), with the installation sequence progressing from the outer edge to the center of the plate, as depicted in Figure 7. This procedure aimed to reduce excess pore water pressure, directing the remnant from the micro-piles group. This installation method was implemented across all configuration models, including K_1 , K_2 , and K_3 .

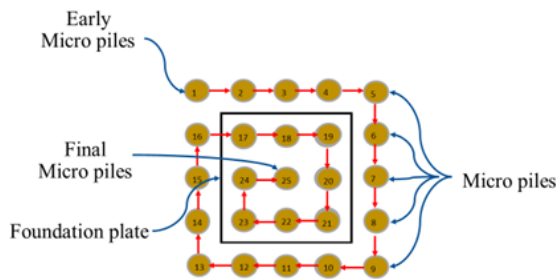


Fig.7 The direction of installing the micro-piles for the number $n_4= 25$.

In this study, micro-piles were limited to withstanding lateral loads, avoiding vertical load bearing from the foundation plate. To achieve the objective, the top end of the micro-piles was installed approximately 0.005 m above the ground level. The measure aimed to prevent the micro-piles from adhering to the foundation plate (Fig.8a) and to ensure the piles were spaced out to minimize variations in settlement (Fig.8b). The installation

method outlined above was designed to ensure that the micro-piles exclusively served to withstand lateral loads. This method was consistent across all numbers of micro-piles ($n_1= 4$; $n_2= 9$; $n_3= 16$; and $n_4= 25$).

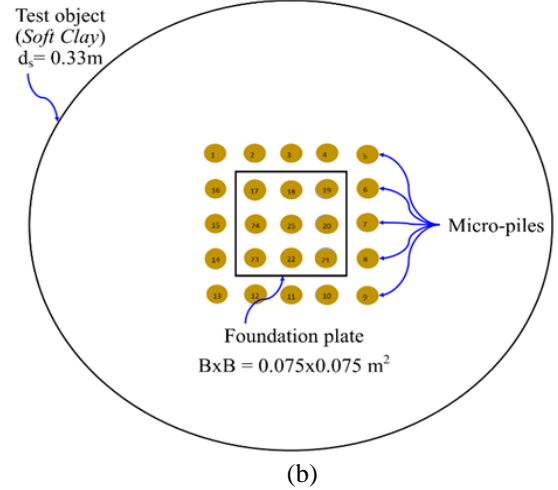
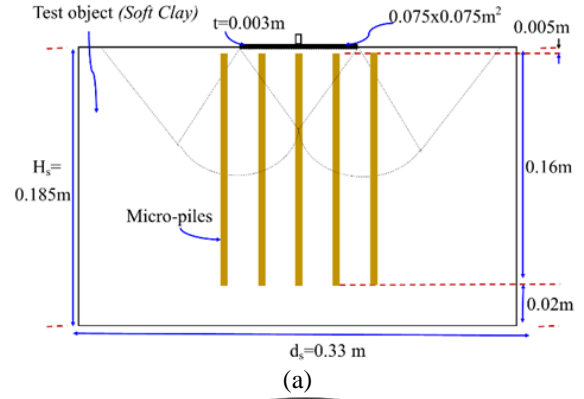


Fig.8 Micro-piles installed for soil shear failure test. (a) Pieces of specimens with $n_4= 25$ and $L_3= 2.13B$. (b) Top view of the micro-piles attached with $n_4= 25$.

Each test object underwent a period referred to as the "waiting period" in a closed and humid environment to restore the soil strength disturbed by the insertion of micro-piles, which caused uneven excess pore water pressure around the pile group. The duration of the waiting period (t) varied depending on the number of micro-piles installed. The waiting period (t) for $n_1= 4$ lasted 1-2 days, for $n_2=9$ took 2-3 days, for $n_3= 16$ was 3-4 days, and for $n_4= 25$ lasted 5-6 days. After the completion of the waiting period, the next step was to conduct the shear failure test.

3.4 Testing

The soil shear failure test aimed to determine the load acting when there was a settlement of $0.1B$ ($P_{0.1B}$), where B represented the width of the foundation ($B= 0.075 \text{ m}$). The experiment was conducted at a vertical loading movement speed of 15 mm/minute [23], ensuring an initial loading (P) of 0 Newton. The analysis concluded upon the occurrence

of significant deformations or failure, at which point the load at 0.1B settlement ($P_{0.1B}$) was recorded. Subsequently, the $q_{ult-empirical}$ of 0.1B could be determined based on the obtained $P_{0.1B}$ from the results.

In this study, a total of 29 test objects were examined, comprising 1 without micro-piles and 28 with various micro-pile configurations (K_1 , K_2 , K_3). The variations in micro-pile lengths, diameters, and installation configurations were detailed in Table 1 through to Table 3.

Table 1. Composition of the number of test objects for configuration of mounting micro-piles (K_1).

Micro-pile	Number of test objects				Micro-pile
length (L)	Number of micro-piles (n)				diameter (d)
m	$n_1=4$	$n_2=9$	$n_3=16$	$n_4=25$	m
$L_1=0.10$	1	1	1	1	$d_1=0.002$
$L_2=0.13$	1	1	1	1	$d_1=0.002$
$L_3=0.16$	1	1	1	1	$d_1=0.002$
$L_3=0.16$	1	1	1	1	$d_2=0.003$
$L_3=0.16$	1	1	1	1	$d_3=0.005$

Table 2. Composition of the number of test objects for configuration of mounting micro-piles (K_2).

Micro-pile	Number of test objects				Micro-pile
length (L)	Number of micro-piles (n)				diameter (d)
m	$n_1=4$	$n_2=9$	$n_3=16$	$n_4=25$	m
$L_3=0.16$	1	1	1	1	$d_1=0.002$

Table 3. Composition of the number of test objects for configuration of mounting micro-piles (K_3).

Micro-pile	Number of test objects				Micro-pile
length (L)	Number of micro-piles (n)				diameter (d)
m	$n_1=4$	$n_2=9$	$n_3=16$	$n_4=25$	m
$L_3=0.16$	1	1	1	1	$d_1=0.002$

The stages of shear failure testing of soil specimens are shown in Figs. 9-16. The testing stages commenced with the preparation of soft clay samples, cutting the prototypes to a certain height, and installing micro-piles as well as plate foundations until the specimens were ready to be subjected to a soil shear failure test. During shear failure test, the load and settlement indicator dials were observed to be zero. The test was stopped until the test specimen experienced maximum shear failure. Furthermore, shear failure analysis was carried out when the settlement reached 0.1 of the foundation B width

(0.1B).



Fig.9 Measurement of the slurry sample height (H_0) to be compressed.



Fig.10 Measurement of the compressed slurry sample height (H_1) with a soft clay load (σ_p') of 114.149 kN/m².



Fig.11 Cutting soft clay soil (H_1) in the test specimen tube with a height (H_{sc}) of 0.185m.



Fig.12 H_{sc} specimen with several micro-piles $n_2= 9$ and configuration K_1 .



Fig.13 H_{sc} test specimen installed on a plate foundation on micro-piles.



Fig.14 Position of the specimen for the soil shear failure test.



Fig.15 The test starts when the load position and deformation are equal to 0.



Fig.16 Shear failure test of soil when the settlement was approximately $0.1B$.

3.5 Analyze Results

Based on Terzaghi's theory, the analysis was carried out under local shear failure conditions across several specimens detailed in Table 1 through to Table 3. The ultimate bearing capacity (q_{ult} -local shear Terzaghi) was obtained from Terzaghi's equation for clay soils with water-saturated conditions and $\phi= 0^\circ$, along with a foundation depth (D_f) of 0 m. Therefore, the ultimate bearing capacity was determined as follows.

$$q_{ult} = 1.3 \cdot c \cdot N_c \quad (1)$$

According to Terzaghi, the internal shear angle ($\phi= 0^\circ$) obtained a bearing capacity factor value (N_c) of 5.7 and for local shear failure conditions, cohesion (c) was used as $2/3 \cdot c_u$ resulting in,

$$q_{ult} = 4.76 \cdot c_u \quad (2)$$

where c_u represented undrained cohesion

The analyzed test results included the ultimate

bearing capacity at 0.1B settlement ($q_{ult-empirical-0.1B}$), which was compared with the ultimate Terzaghi bearing capacity based on local shear failure conditions ($q_{ult-local\ shear\ Terzaghi}$). This was called the ratio of increasing the ultimate bearing capacity of shallow foundations after installing micro-pile reinforcement ($R_{q_{ult-mp}}$). The comparison between the two ($R_{q_{ult-mp}} = q_{ult-empirical-0.1B} / q_{ult-local\ shear\ Terzaghi}$) for each configuration (K_1, K_2, K_3) with variations in parameters (n, d, L) was analyzed to determine the most effective configuration for increasing the ultimate bearing capacity at 0.1B settlement based on SNI 2017 [24].

4. RESULT AND DISCUSSION

Figures 17 to 19 indicated the outcome of laboratory experiments investigating the influence of micro-pile number, length, diameter, and installation configuration on the increase in ultimate bearing capacity ratio at a 0.1B reduction ($R_{q_{ult-mp}} = q_{ult-empirical-0.1B} / q_{ult-local\ shear\ Terzaghi}$). Based on the results, the ultimate bearing capacity ratio during a settlement of 0.1B ($=R_{q_{0.1B}}$) was observed to be 1.1. This implied that the capacity of the test during the settlement without micro-piles ($n=0$) and the capacity of Terzaghi's theory at local shear failure were almost identical. The result showed conformity between the experimental test and Terzaghi's theory. This finding was also supported by previous research, including Piamat K., et al. [25], as well as Isnaniati and Mochtar [26].

The impact of increasing the number (n) of micro-piles installed beneath shallow foundations on enhancing the ultimate bearing capacity was presented in Figs. 17 to 19. Across various lengths, diameters, and installation configurations, the ultimate bearing capacity ratio at a settlement of 0.1B ($R_{q_{ult-mp}} = q_{ult-empirical-0.1B} / q_{ult-local\ shear\ Terzaghi}$) consistently rises with an increasing number of (n) micro-piles. This phenomenon was attributed to the greater shear strength provided by a larger number of piles, resulting in an augmentation of the ultimate bearing capacity, as suggested by Mochtar [27].

The effect of the number of micro-piles (n) on the increase in ultimate bearing capacity ratio ($R_{q_{ult-mp}}$) with variations in the length (L) was observed in Fig.17. The graph showed that the longer length of the micro-piles (L) correlated significantly with an increase in the ratio value of $R_{q_{0.1B}}$. This phenomenon was caused by extending the length of micro-piles which could increase the area of resistance or lateral reaction. Due to the expansion, the ability to withstand lateral forces will be increased along with the empirical ultimate bearing capacity ($q_{ult-empirical-0.1B}$) and the $R_{q_{0.1B}}$. The most significant increase in $R_{q_{0.1B}}$ occurred in the longest micro-piles ($L_3 = 2.13B$) with 25 numbers of micro-piles (n). The results correlated with previous research conducted

by Rusdiansyah et al. [10,11].

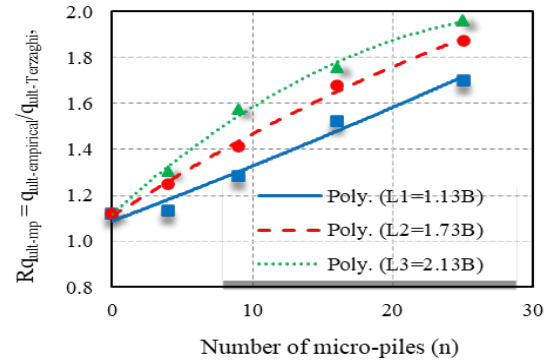


Fig.17 Effect of the number of micro-piles (n) on the ultimate bearing capacity ratio when the settlement was 0.1B (R_q) with variations in the length (L) in soft clay soil, $K_1=0.67B$, and $d_1=0.03B$.

The effect of the number of micro piles (n) on increasing the ultimate bearing capacity ratio of shallow square foundations ($R_{q_{0.1B}}$) with variations in micro piles diameter (d) was presented in Fig.18. The $R_{q_{0.1B}}$ value for all pile diameters ($d_1=0.03B$, $d_2=0.04B$, $d_3=0.07B$) increased with a rising number (n) of micro-piles. However, the most substantial increase in $R_{q_{0.1B}}$ occurred when the cone diameter was 0.04B. This was attributed to the fact that when the diameter exceeds 0.04B, the micro-piles become overly robust. Furthermore, the shear failure of the soil becomes primarily determined by the soil's strength, thereby preventing a significant increase in R_q and even leading to a decrease.

For cones with diameters $d_2=0.04B$ and $d_3=0.07B$, the $R_{q_{0.1B}}$ values were nearly identical for the same number of micro-piles. Conversely, for the micro-pile with a diameter (d_1) of 0.03B, the increase in $R_{q_{0.1B}}$ was minimal compared to piles with diameters (d_2) of 0.04B and (d_3) of 0.07B with the same number of micro-piles, as depicted in Fig.18. This discrepancy arises from the smaller diameter, resulting in lesser lateral force absorption and a minor increase in R_q .

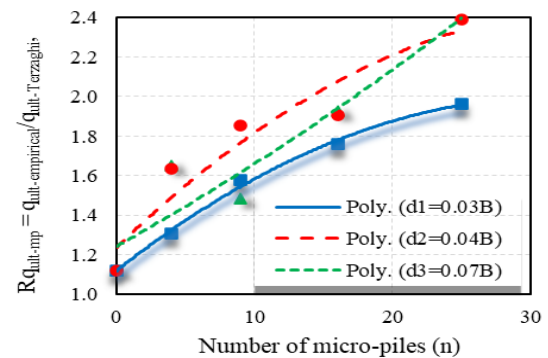


Fig.18 Effect of the number of micro-piles (n) on the ultimate bearing capacity ratio when the settlement

was 0.1B (Rq) with variations in diameter (d) in soft clay soil, $K_1=0.67B$, and $L_3=2.13B$.

Figure 19 illustrates the impact of the configuration of placing micro piles (K) under the foundation on increasing the ultimate bearing capacity ratio ($R_{q0.1B}$) for shallow square foundations. The $R_{q0.1B}$ values for all micro-pile mounting configurations ($K_1=0.67B$, $K_2=B$, and $K_3=1.33B$) increase with increasing number (n) of micro-piles. However, the increase in $R_{q0.1B}$ is not significant for micro piles installed outside the foundation ($K_3=1.33B$) compared to those installed inside and to the edge of the foundation ($K_1=0.67B$ and $K_2=B$). This is because, in soft clay soil the collapse that occurs is Local Shear Failure so the soil that experiences shifting is located only under the shallow foundation. This condition is for $K_1/B=0.67$ to $K_2/B=1$. If $K_3/B>1$, the part of the micro piles, which is outside the foundation, can be considered not to have experienced soil movement. So the overall shear resistance of the soil decreases. This is by the collapse model of Terzaghi's theory in 1943.

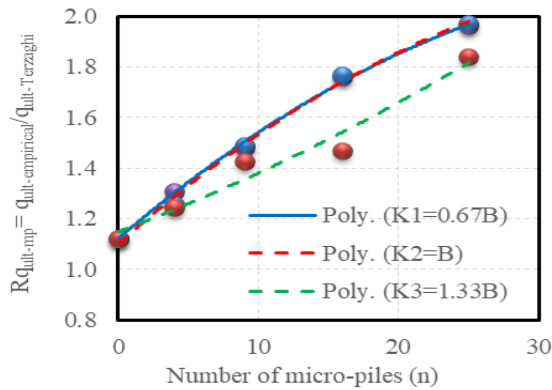


Fig.19 Effect of the number of micro piles (n) on the ultimate bearing capacity ratio when the settlement was 0.1B (Rq) with variations in the installation configuration of micro piles (K) in soft clay soil, $L_3=2.13B$, and $d_1=0.03B$.

The ultimate bearing capacity equation for micro piles (q_{ult-mp}) was developed based on Terzaghi's theory in 1943. The equation was derived by multiplying the ultimate bearing capacity of Terzaghi's theory at local shear failure with the capacity ratio at a decrease of 0.1B. Analyzing the results depicted in Figs. 17 to 19, data from configurations K_1 and K_2 were selected for $L_3=2.13B$ and $d_1=0.03B$ to obtain the equation for the ultimate bearing capacity ratio at a decrease of 0.1B ($R_{q0.1B}$), as shown in Fig.20. The equation was represented as $R_{q0.1B}=1.1112+0.0517n-0.0007n^2$, where n denoted the number of micro-piles, and $R_{q0.1B}$ represented the ratio $q_{ult-empirical}/q_{ult-Terzaghi}$, local failure. The magnitude of $q_{ult-Terzaghi}$ local failure was calculated as $4.94c_u$, with c_u

being 20.692 kN/m^2 , and $q_{ult-empirical}$ was determined through shear failure testing of the soil with a settlement of 0.1B.

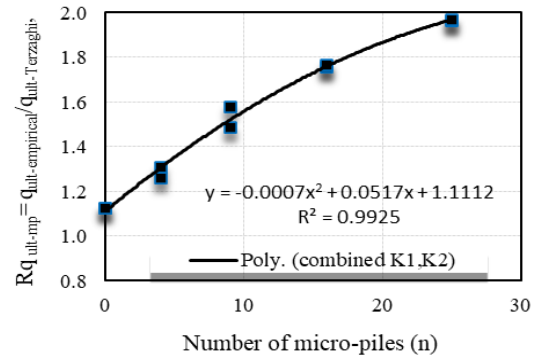


Fig.20 Impact of the number of micro-piles on the ultimate bearing capacity ratio when the settlement was 0.1B (Rq) in soft clay soil, for the combination K_1 , K_2 with $d_1=0.03B$; $L_3=2.13B$.

The results of this study showed that micro-piles with certain variations in length, number, and installation configuration can increase the foundation's bearing capacity. Several studies, as indicated by Park H et al. [28], have validated the efficacy of using micro-piles under shallow foundations, considering factors such as foundation thickness, depth, installation configuration, and the number of micro-piles. Park's study found that micro-piles could reduce settlement and bending moments in shallow foundations. Remarkably, the centrifuge test used a pile system parallel to the investigation conducted in this study, yielding results contributing to settlement reduction and enhanced bearing capacity.

Eslami et al. [29] conducted a comparative study focusing on the area where unconnected pile rafts were installed, similar to the system examined in this study. The results showed the effective role of raft piles installed separately in mitigating settlement, particularly when concentrated in the central and edge regions of the foundation (K_1 and K_2). The configuration of pile installation (K) in the study significantly reduced settlement, specifically when concentrated within 15-25% of the foundation area.

Numerical investigations conducted by various scholars [30,31] using 3D element analysis have explored Disconnected Piled Raft (DPR) interactions and Load Transfer Loads (LTP) compared to piles connected to rafts. These studies found that the DPR system can effectively minimize settlement and transfer loads to deeper soil layers, thereby influencing the soil-bearing capacity. The findings emphasized that micro-piles beneath shallow foundations can enhance soil-bearing capacity and increase the ratio, contingent upon factors such as number, length, and configuration of placement (K),

thereby corroborating the outcomes of the previous study with the findings of this study.

5. CONCLUSIONS

The following conclusion can be observed based on the data and analysis of the results presented. These findings provided valuable insights into the effectiveness of micro-piles in enhancing the bearing capacity of shallow foundations.

- a. As the number of micro-piles ($n_1=4$, $n_2=9$, $n_3=16$, $n_4=25$) increases, the ultimate bearing capacity ratio at 0.1B settlement ($R_{q_{ult-mp}} = q_{ult-empirical}/q_{ult-local}$ shear Terzaghi) also expanded. The greater the number of micro-piles, the higher the increase in $R_{q_{0.1B}}$.
- b. The length of the crevice significantly influenced the increase in $R_{q_{0.1B}}$, with the most substantial increase observed in the longest micro-piles ($L_3 = 2.13B$) when coupled with a larger number of micro-piles ($n_4 = 25$).
- c. The largest increase in $R_{q_{0.1B}}$ occurred when the micro-piles diameter ($d_2 = 0.04B$) and the number of micro-piles ($n_4 = 25$) were at the maximum.
- d. Mounting micro-piles in the K_3 configuration of 1.33B did not yield a significant increase in $R_{q_{0.1B}}$ value compared to configurations K_1 and K_2 , regardless of the number (n) of micro-piles used.
- e. The ultimate bearing capacity ratio of micro-piles ($R_{q_{ult-mp}}$) decreased at 0.1B, when the piles were configured from the middle to the edge of shallow foundations (K_1 to K_2). L_3 and d_1 in soft clay soil were determined as $R_{q_{ult-mp}} = 1.1112 + 0.0517n - 0.0007n^2$, where n represented the number of micro-piles.

6. REFERENCES

- [1] Terzaghi K., Peck R., and Mesri G., Soil Mechanics in Engineering Practice.pdf, John Wiley and Sons Singapore, 1996, pp.1-534.
- [2] Braja M. Das., Shallow Foundations Bearing Capacity and Settlement, Taylor and Francis Group, 2017, pp.1-401.
- [3] Tsukada Y., Tsubokawa Y., Otani Y., Lin You G., Mechanism of Bearing Capacity of Spread Footings Reinforced with Micro Piles, Journal Soils and Foundations, Vol.46, No.534, 2006, pp.367-376.
- [4] Suroso., and Harimurti., Alternative for Reinforcement of Soft Clay Soil Using Micro Piles with Variations Length and Diameter of Micro-Piles, Civil Engineering Journal, Vol.2, No.1, 2008, pp.47-61.
- [5] Alnuaim A. M., and Naggar M. H. E., Numerical Investigation of the Performance of Micropiled Rafts in Sand, Comput Micro Piled Rafts in Sand, Comput Geotech, Vol.77, 2016, pp.91-105.
- [6] Alnuaim A. M., and Naggar M. H. E., Performance of Micro Piled Rafts in Clay Numerical Investigation, Comput Geotech, Vol.99, Oktober, 2018, pp.42-54.
- [7] Wen L., Kong G., Abuel-Naga Q. L., and Zhang Z., Rectification of Tilted Transmission Tower Using the Micropile Underpinning Method, Journal of Performance of Constructed Journal Facilities, Vol.34, No.1, 2020, pp.1-7.
- [8] Shah I. A., Zaid M., Farooqi M. A., and Ali K., Numerical Study on Micropile Stabilized Foundation in Flyash, Indian Geotechnical Journal, Vol.51, No.5, 2021, pp.1099-1106.
- [9] Hasheminezhad A., and Bahadori H., On the Deep Soil Mixing Method in the Mitigation of Liquefaction Induced Bearing Capacity Degradation of Shallow Foundations, Geomechanics and Geoengineering, Vol.17, No.1, 2022, pp.334-346.
- [10] Rusdiansyah., Mochtar I. B., dan Mochtar N. E., Effect of Burrow Depth, Spacing, and Number of Micro-Piles in Increasing the Shear Resistance of Soft Soil Based on Laboratory Modeling, Journal info technic, 2015, pp.289-302.
- [11] Rusdiansyah, Mochtar I. B., and Mochtar N.E., Study on the Increase of Shear Resistance of Soft Soil Due to Vertical Piles Reinforcement Based on Modelling in the Laboratory, International Journal of Applied Engineering Research, Vol.11, No.8, 2016, pp.5934-5942.
- [12] Abbas Q., Choi W., Kim G., Kim I., and Lee J., Characterizing Uplift Load Capacity of Micro Piles Embedded in Soil and Rock Considering Inclined Installation Conditions, Computer Geotech, Vol.132, August 2020, pp.1-12.
- [13] Bahtiar E. T., Imanullah A. P., Hermawan D., Nugroho N., and Abdurachman, Structural Grading of Three Sympodial Bamboo Culms (Hitam, Andong, and Tali) Subjected to Axial Compressive Load, Engineering Struct, Vol.181, 2019, pp.233-245.
- [14] Kumar D., and Mandal A., Review on Manufacturing and Fundamental Aspects of Laminated Bamboo Products for Structural Application Constr Build Mater, Vol. 348, 2020, pp.1-6.
- [15] Ye F., and Fu W., Physical and Mechanical Characterization of Fresh Bamboo for Infrastructure Projects, 2017, pp.1-10.
- [16] Lambe T. W., Soil Mechanics, in The Engineering Handbook, Second Edition, 1969, pp.1-7.
- [17] Brown., Engineering and Design Bearing Capacity of Soils, ASCE, 1994, pp.1.1-5.42
- [18] Alfani A. A., Sugianto D. N., and Indrayanti E., Physical Model Affects Armor Cylinder

- Vertical Breakwater, Indonesian Journal of Oceanography, Vol.4, No.1, 2022, pp.23–35.
- [19] Esmailpor P., Mamazizi A., and Madabhushi G. S. P., An Overview of the Model Container Types in Physical Modeling of Geotechnical Problems, Soil Dynamics and Earthquake Engineering, Vol.168, July, 2022, pp.1-32.
- [20] Issakulov A., Omarov A., Zhussupbekov S., Mussakhanova, and Issakulov B, Investigation of the Interaction of the Bored Micro Pile by DDS (Fdp) Technology With the Soil Ground, International Journal of GEOMATE, Vol. 24, Issue 105, 2023, pp.11–17.
- [21] Isnaniati., Contribution of Pole Cross Section Shape to the Maximum Load Accepted Foundation for Foundation Planning on Clay Soil CPT Surabaya Data, Aggregate Journal, Vol.2, No.1, 2017, pp.21–27.
- [22] Munawir A., Bearing Capacity Improvement of Shallow Foundation on Multilayered Geogrid Reinforced Sand, International Journal of GEOMATE, Vol.18, Issue 69, 2020, pp.216-223.
- [23] ASTM International, Designation C 293-94: This standard has either been superseded and replaced by a new version or discontinued Contact ASTM International (www.astm.org) for the latest information. Standard Test Method for Flexural Strength of Concrete pp.1-3.
- [24] National Standardization Agency, Geotechnical design requirements, BSN Jakarta, Vol.8460, 2017, pp.1-323.
- [25] Piyasawat K., Nuntasarn R., Hormdee D., and Punrattanasin P., Bearing Capacity of Shallow Foundation on Collapsible Khonkaen Loess, International Journal of GEOMATE, Vol.20, Issue 80, 2021, pp.159–167.
- [26] Isnaniati, and Mochtar I. B., Increasing the Bearing Capacity of Shallow Foundations on on Soft Soil After the Installation of Micro Piles, Journal of the Civil Engineering Forum, Juli, 2023, pp.227–238.
- [27] Mochtar N. E., Soil Improvement, ITS press, 2012, pp.1-143.
- [28] Park H., Ko. K., Song Y., Jin S., Ha S., Kim D., Centrifuge Modeling of Disconnected Piled Piled Raft Using Vertical Pushover Test, Acta Geotech, Vol.15, No.9, 2020, pp.2637–2648.
- [29] Eslami A., Veiskarami M., and Eslami M., Study on Optimized Piled-Raft Foundations (PRF) Performance with Connected and Non-Connected Piles Three se Histories, International Journal of Civil Engineering, Vol.10, no.2, 2012, pp.100–111.
- [30] Tradigo F., Pisanò F., Prisco C., and Mussi A., Non-Linear Soil Structure Interaction in Disconnected Piled Raft Foundations, Computer Geotech, Vol.63, 2015, pp.121–134.
- [31] Hor B., Song M. J., Jung M. H., Song Y., and Pak Y. H., A 3D FEM analysis on ence on Soil Mechanics and Geotechnical Engineering, ARC, January 2015, pp.1238-1243.

Copyright © Int. J. of GEOMATE All rights reserved, including making copies, unless permission is obtained from the copyright proprietors.
